The Influence of Particle Size and Multiple Apoprotein E–Receptor Interactions on the Endocytic Targeting of β-VLDL in Mouse Peritoneal Macrophages

Ira Tabas,*‡ Jeffrey N. Myers,§ Thomas L. Innerarity,¶ Xiang-Xi Xu,* Kay Arnold,¶ Janet Boyles,¶ and Frederick R. Maxfield§‖

Departments of *Medicine, ‡Anatomy and Cell Biology, §Pathology, and ‖Physiology, Columbia University, New York 10032; and ¶Gladstone Foundation Laboratories for Cardiovascular Disease, Departments of Pathology and Medicine, Cardiovascular Research Institute, University of California, San Francisco, San Francisco, California 94140-0608

Abstract. Low density lipoprotein (LDL) and β-very low density lipoprotein (β-VLDL) are internalized by the same receptor in mouse peritoneal macrophages and yet their endocytic patterns differ; β-VLDL is targeted to both widely distributed and perinuclear vesicles, whereas LDL is targeted almost entirely to perinuclear lysosomes. This endocytic divergence may have important metabolic consequences since β-VLDL is catabolized slower than LDL and is a more potent stimulator of acyl-CoA/cholesterol acyl transferase (ACAT) than LDL. The goal of this study was to explore the determinants of β-VLDL responsible for its pattern of endocytic targeting. Fluorescence microscopy experiments revealed that large, intestinally derived, apoprotein (Apo) E-rich β-VLDL was targeted mostly to widely distributed vesicles, whereas small, hepatically derived β-VLDL was targeted more centrally (like LDL). Furthermore, the large β-VLDL had a higher ACAT-stimulatory potential than the smaller β-VLDL. The basis for these differences was not due to fundamental differences in the means of uptake; both large and small β-VLDL were internalized by receptor-mediated endocytosis (i.e., not phagocytosis) involving the interaction of Apo E of the β-VLDL with the macrophage LDL receptor. However, large β-VLDL was much more resistant to acid-mediated release from LDL receptors than small β-VLDL. Furthermore, partial neutralization of the multiple Apo Es on these particles by immunotitration resulted in a more perinuclear endocytic pattern, a lower ACAT-stimulatory potential, and an increased sensitivity to acid-mediated receptor release. These data are consistent with the hypothesis that the interaction of the multivalent Apo Es of large β-VLDL with multiple macrophage LDL receptors leads to a diminished or retarded release of the β-VLDL from its receptor in the acidic sorting endosome which, in turn, may lead to the widely distributed endocytic pattern of large β-VLDL. These findings may represent a physiologically relevant example of a previously described laboratory phenomenon whereby receptor cross-linking by multivalent ligands leads to a change in receptor targeting.

Ligands and receptors internalized by receptor-mediated endocytosis may undergo a variety of cellular itineraries, including targeting of both ligand and receptor to lysosomes, recycling of both ligand and receptor to the cell surface, or targeting of the ligand to lysosomes and receptor to the cell surface after ligand–receptor uncoupling in sorting endosomes (13). A major goal in this area of research has been to elucidate ligand–receptor properties that may influence the endocytic itinerary and thus the intracellular metabolism of individual ligands and their receptors. Along these lines, several groups have reported that the cross-linking of specific receptors by polyvalent antibody or multivalent ligands on gold particles can alter the endocytic itinerary of these ligands and their receptors (1, 14, 26, 29, 32, 38).

Research from our laboratories has revealed that two different lipoprotein ligands for the same receptor, the macrophage low density lipoprotein (LDL) receptor, have divergent endocytic pathways in mouse peritoneal macrophages: LDL is rapidly targeted to perinuclear lysosomes near the center of the cell, whereas a significant portion of the β-very low density lipoprotein (β-VLDL) is found in more widely distributed vesicles whose interiors are relatively electron lucent when viewed by EM (37). This finding has two potential areas of importance. Firstly, an understanding of the

1. *Abbreviations used in this paper*: ACAT, acyl-CoA/cholesterol acyl transferase; Apo, apoprotein; CE, cholesteryl ester; DiI, 1,1′-dioctadecyl-3,3,3′,3′-tetramethyl-indocarbocyanine perchlorate; LDL, low density lipoprotein; VLDL, very low density lipoprotein.

© The Rockefeller University Press, 0021-9525/91/12/1547/14 $2.00

mechanism of the endocytic divergence of these two ligands may help elucidate ligand properties that are important in determining endocytic itineraries. Secondly, the divergent endocytic targeting of LDL and β-VLDL in macrophages may have important physiological consequences related to their intracellular metabolism. In particular, β-VLDL is degraded more slowly and stimulates the intracellular cholesterol esterification enzyme acyl-CoA/cholesterol acyl transferase (ACAT) more potently than LDL in these cells (37). Since macrophages which have accumulated large amounts of ACAT-derived cholesteryl ester (CE) ("foam cells") are a prominent feature of atherosclerotic lesions (8, 10, 34) and since β-VLDL is known to be an "atherogenic" lipoprotein (25), our studies on the endocytosis of β-VLDL in macrophages may contribute to our understanding of mechanisms of atheroma foam cell formation.

The goal of the current study was to explore the properties of β-VLDL particles that are responsible for their distinct endocytic pathway (and metabolism) in macrophages. The data revealed that not all β-VLDL particles behaved similarly: large apoprotein (Apo) E-rich, intestinally derived β-VLDL were targeted mostly to widely distributed vesicles, whereas small, hepatically derived β-VLDL were targeted more centrally (like LDL). These endocytic differences were associated with an important metabolic difference as well: large β-VLDL stimulated ACAT greater than small β-VLDL. Several possible explanations for these endocytic (and ACAT) differences were explored, and the data suggest that binding of large β-VLDL via multiple Apo E subunits to macrophage LDL receptors, which probably leads to receptor cross-linking, results in an alteration of the pattern of endocytosis and perhaps ACAT stimulation. Thus, these findings may represent a physiologically important example of the effects of ligand multivalency and receptor cross-linking on ligand-receptor endocytic routing.

Materials and Methods

Cells

Peritoneal macrophages from unstimulated female ICR mice (25–35g; Harlan Sprague Dawley, Inc., Indianapolis, IN) were plated onto coverslip-bottom dishes and preincubated for 2 d in DME/10% lipoprotein-deficient serum (vol/vol) as previously described (37). In certain experiments, the LDL receptor on the cells was partially down-regulated by adding to the preincubation medium 5 μg/ml acetyl-LDL (11) plus 1 μg/ml of the ACAT inhibitor, compound 58-035 (3-[decyldimethylsilyl]-*N*-[2-(4-methylphenyl)-1-phenylethyl] propanamide) (31) (generously provided by Dr. John Heider, Sandoz, Inc., East Hanover, NJ). All experiments were performed on day 3.

Lipoproteins and Proteins

LDL was prepared as previously described (37). $d < 1.006$ lipoproteins from cholesterol-fed rabbits and cholesterol-fed dogs were prepared by ultracentrifugation at $d = 1.006$ g/ml (17). These $d < 1.006$ lipoproteins, which contain mostly β-VLDL but also some pre-β-VLDL, will be referred to as simply "β-VLDL." Aggregated LDL was prepared by vigorously vortexing LDL for 30 s as described by Khoo et al. (18).

The lipoproteins were labeled with 1,1'-dioctaolecyl-3,3,3',3'-tetramethylindocarbocyanine perchlorate (DiI) (Molecular Probes Inc., Junction City, OR) by the method of Pitas et al. (30) and with ^{125}I (IMS.30; carrier-free; Amersham Corp., Arlington Heights, IL) using iodine monochloride as described in detail previously (12). The lipoproteins were labeled with ^{3}H-labeled CE by transfer (via semipurified CE transfer protein) of ^{3}H-CE from ^{3}H-CE-HDL donor (36).

Canine β-VLDL lipids and proteins were analyzed for lipid composition (cholesterol, triglycerides, and phospholipid) by analysis on a Spectrum high performance diagnostic system (Abbott Laboratories, Diagnostic Div. Department, Abbott Park, IL) and for protein content by the method of Lowry et al. (24). Negative-stain EM of the β-VLDL was carried out as described by Boyles et al. (4). Canine β-VLDL was fractionated by gel filtration chromatography on BioGel A-150m agarose beads (Bio-Rad Laboratories, Richmond, CA) in saline-EDTA (0.15 M NaCl, 0.01% EDTA) (9). Each fraction was analyzed by absorbance at 280 nm and by colorometric cholesterol assay (Boehringer Mannheim Diagnostics, Inc., Houston, TX) to determine peaks.

α_2-Macroglobulin (α_2M) was purified, converted to the receptor-binding form, and conjugated to FITC as previously described (33).

Antibodies

Polyclonal rabbit anti-bovine adrenal LDL receptor antibody was prepared as described by Schneider et al. (35) and Beisiegel et al. (3). Monoclonal antibodies against Apo B100 (4G3, IgG_{2a}) and Apo E (1D7, IgG_1) were kindly provided by Drs. Ross Milne and Yves Marcel (Clinical Institute of Montreal, Montreal, Canada) and were characterized previously (27, 28). The polyclonal and monoclonal antibodies were purified by protein A-Sepharose chromatography. As a control (i.e., irrelevant) antibody, we used rabbit IgG against dinitrophenyl-BSA or mouse monoclonal IgG_1 against clathrin heavy chain. Anti-Apo E (1D7) Fab fragments were made by digesting the intact IgG with immobilized papain and then separating the Fab fragments from Fc fragments and undigested IgG using an immobilized protein A column (ImmunoPure Fab preparation kit, Pierce Chemical Co., Rockford, IL).

Video Intensification Fluorescence Microscopy

Cells were incubated, washed, formaldehyde fixed, and viewed by fluorescence microscopy as described previously (37) and as indicated in the individual figure legends. Images were digitized (Gould-Vicom IP 9000 image processor, Vicom, Inc., Fremont, CA) and photographs were produced (Polaroid Freeze Frame, Polaroid Corp., Cambridge, MA).

Individual cells from double-labeled experiments (fluorescein-α_2M and DiI-labeled lipoproteins) were analyzed for overlap of fluorescent vesicles as follows: autofluorescence and out-of-focus background fluorescence in the digitized images were removed by applying a 32 × 32 pixel (5.5 × 5.5 μm) median filter to a digitized image, and subtracting the result from the original image. Individual endocytic vesicles were detected as contiguous groups of pixels with an intensity greater than a specified threshold. Pixels not removed by background subtraction were eliminated by deleting from a vesicle any pixel with an intensity <50% of the maximum intensity of the vesicle. This procedure separates close but distinct vesicles while retaining an accurate relative measure of intensity for each vesicle (6). Next, images were aligned to correct for the small relative offset of the images resulting from the use of different filter sets for fluorescein and DiI fluorescence. In addition, a few cells failed to endocytose significant amounts of α_2M. To avoid underestimating the amount of overlapping vesicles, α_2M-negative cells were individually removed from both images in the double-label pair. Finally, these pairs of processed images of endosomes were used to determine whether individual endosomes contained both labeled ligands. If <25% of the pixels in a β-VLDL-containing endosome overlapped with an α_2M-containing endosome, the endosome was considered to lack α_2M. The number and total intensity of nonoverlapping endosomes was determined, and expressed as a fraction of the total number or total intensity of endosomes in an image. Several images were analyzed for each experimental condition, with each image containing 3–5 cells.

SDS-PAGE

β-VLDL fractions were dialyzed against 0.01% EDTA, lyophilized, delipidated with chloroform/methanol, and resolubilized in SDS sample loading buffer according to the method of King and Laemmli (19). The samples (10 μg) were electrophoresed under reducing conditions on a 5–20% gradient SDS-polyacrylamide gel. The protein bands were stained with Coomassie blue, and the wet gels were scanned on a densitometer (model GS300, Hoefer Sci. Instrs., San Francisco, CA). The data were integrated using gel scanner software (DataLab, St. Jude's Children's Hospital, Memphis, TN) on an Apple computer. The molecular mass markers used were lysozyme (14.3 kD), trypsin inhibitor (21.5 kD), carbonic anhydrase (30 kD), ovalbumin (46 kD), BSA (69 kD), phosphorylase b (97 kD), and myosin (200 kD).

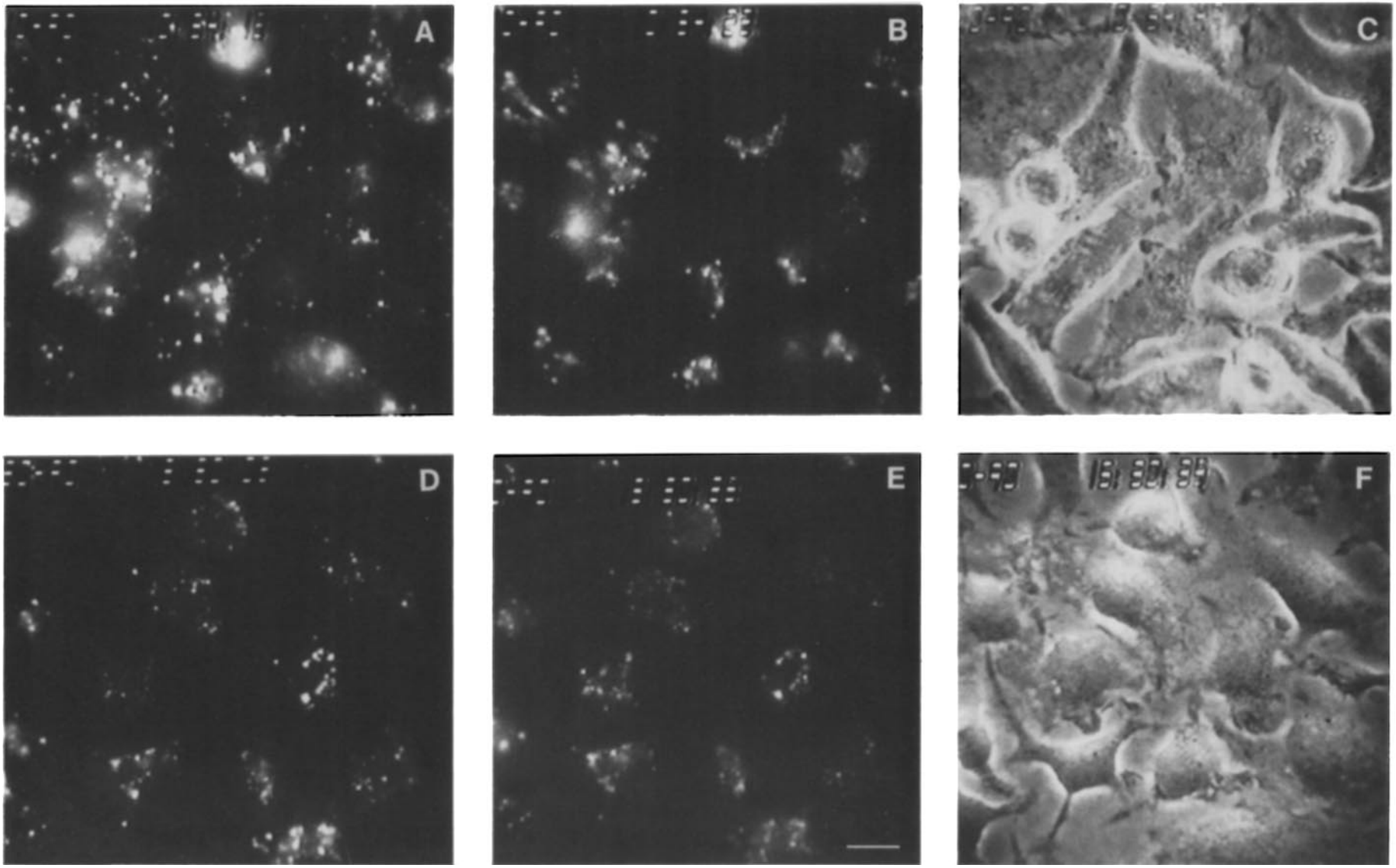

Figure 1. Double-label fluorescence and phase microscopy of macrophages incubated with DiI-canine β-VLDL plus fluorescein-α_2M or with DiI-LDL plus fluorescein-α_2M. Macrophages were incubated with DME/0.2% BSA containing DiI-canine β-VLDL (5 μg/ml) plus fluorescein-α_2M (100 μg/ml) for 6 min and then chased in the absence of ligands for 4 min. The cells were then fixed and viewed by fluorescence microscopy to visualize either DiI (β-VLDL) (*A*) or fluorescein (α_2M) (*B*); the phase image is shown in *C*. In a separate experiment, cells were incubated with DiI-LDL (20 μg/ml) plus fluorescein-α_2M (100 μg/ml) as above; the LDL pattern is shown in *D*, the α_2M pattern is shown in *E*, and the phase image is shown in *F*. Bar, 10 μm.

Other Assays

^{125}I-lipoprotein degradation and binding assays and whole cell ACAT assays were performed as previously described (37). The cellular content of lipoprotein-derived [^{3}H]cholesterol was determined by TLC analysis of cellular unesterified and esterified [^{3}H]cholesterol as previously described (37). Protein was measured by the method of Lowry et al. (24).

Results

Characterization and Endocytic Patterns of Canine β-VLDL Subfractions

Research from our laboratories has recently demonstrated that endocytosis of rabbit β-VLDL by mouse peritoneal macrophages resulted in a pattern of endocytosis distinct from that of LDL; the LDL was rapidly targeted to perinuclear lysosomes whereas much of the rabbit β-VLDL was targeted to more widely distributed vesicles (37). During some initial experiments designed to elucidate the properties of β-VLDL responsible for its distinct pattern of endocytic targeting, occasional rabbit β-VLDL preparations were noted to give a more "mixed" pattern of endocytosis (i.e., central plus widely distributed) than the mostly widely distributed pattern of other rabbit β-VLDL preparations. In further experiments, β-VLDL obtained from cholesterol-fed dogs was found to consistently give a "mixed" pattern of endocytosis. The double-label fluorescence micrographs shown in Fig. 1 compare the endocytic patterns of DiI-canine β-VLDL and DiI-LDL with that of fluorescein-α_2M, which, like LDL, is rapidly targeted to central lysosomes (see reference 37 and below) and thus can serve as a reference for comparison of endocytic patterns. The comparison of the DiI-canine β-VLDL pattern (Fig. 1 *A*) with the fluorescein-α_2M pattern (Fig. 1 *B*) showed that the canine β-VLDL pattern contained many central vesicles that overlapped with fluorescein-α_2M as well as some nonoverlapping, widely distributed vesicles; the phase photomicrograph of these cells is shown in Fig. 1 *C*. This comparison was in contrast to the comparison of DiI-LDL (Fig. 1 *D*) with fluorescein-α_2M (Fig. 1 *E*), where the overlap in fluorescence was almost complete. Thus, canine β-VLDL was targeted to both central lysosomes and more widely distributed vesicles in mouse peritoneal macrophages. This pattern of endocytosis was different from those of LDL and α_2M, which were almost completely targeted to central lysosomes, and from most preparations of rabbit β-VLDL, which were targeted much more to the widely distributed vesicles (37).

The "mixed" endocytic pattern of canine β-VLDL was further explored with the idea that such studies might reveal properties of β-VLDL which were important in its targeting to the widely distributed vesicles. Along these lines, experiments were designed to determine whether this heterogeneous pattern was related to another area in which canine β-VLDL heterogeneity had been demonstrated: particle size and origin. Cholesterol-fed dogs give rise to large, intestinally derived β-VLDL particles as well as smaller, hepatically derived particles (9). Therefore, DiI-labeled canine β-VLDL was size fractionated using gel filtration chromatography (BioGel A-150m), and the fractions were examined for their endocytic patterns and ACAT-stimulatory potential.

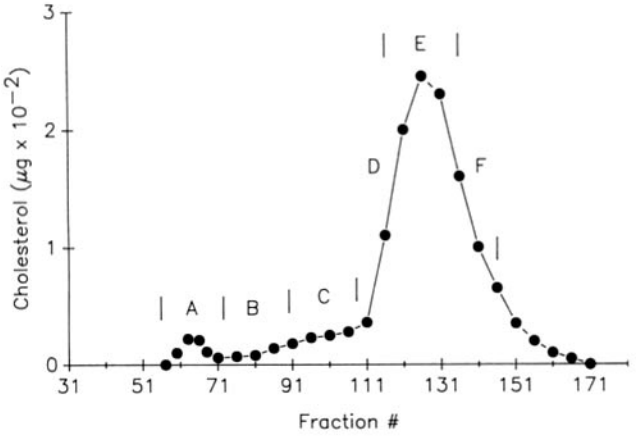

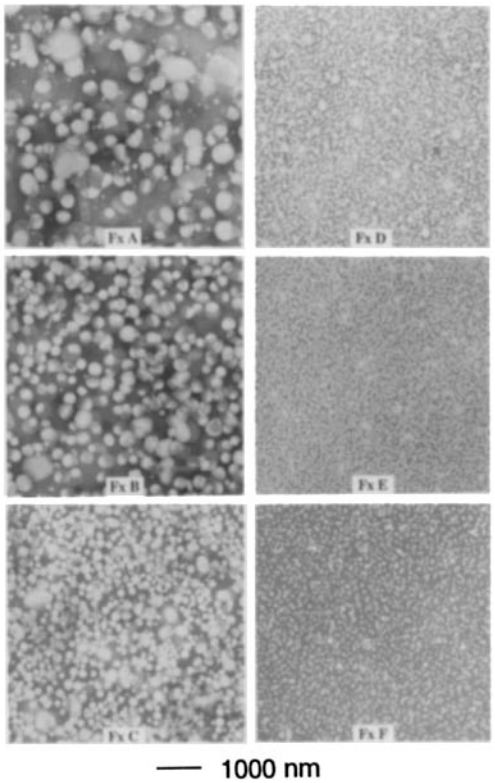

Figure 2. Gel filtration chromatography of DiI-labeled canine β-VLDL. (*Left*) DiI-labeled canine β-VLDL was loaded onto a 3.2 × 90-cm BioGel A-150m gel filtration column, and 4.5-ml fractions were collected. The cholesterol content of each fraction was assayed using a standard colorimetric assay. The fractions were pooled as indicated (*A–F*). (*Right*) Negative-stain electron microscopy of canine β-VLDL size subfractions *A–F*. *Fx*, fraction. Bar, 1,000 nm.

Fig. 2 shows the gel filtration profile of DiI-labeled canine β-VLDL. There was a small peak of cholesterol-containing material in the void volume (fraction A) and a larger peak of material in the included volume (fractions D–F). Fractions in between these two peaks (B and C) were also harvested as indicated in the figure. Fig. 2 shows negative-stain electron micrographs of each of the six fractions (A–F) from the gel filtration chromatography. Fractions A and B had the characteristic appearance of chylomicron remnant particles (white eccentric core and gray periphery), with the particles in fraction A measuring ~350–600 nm in diameter and those in fraction B measuring ~230–400 nm. Fractions C–F did not have the remnantlike appearance and measured ~150–230 nm (C), ~100–150 nm (D), ~75–100 nm (E), and ~50–75 nm (F).

Further characterization of the canine β-VLDL subfractions is shown in Table I. Compared to the smaller β-VLDL, the larger particles have a higher triglyceride content and lower protein, cholesterol, and phospholipid contents. In addition, Coomassie-stained 5–20% gradient SDS-PAGE of canine holo–β-VLDL (which consists mostly of smaller β-VLDL, see above) and pooled fractions D–F revealed that these fractions were enriched in Apo B-100 (data not shown), consistent with the hepatic origin of small β-VLDL. In contrast, the Apo B bands of fractions A–C were enriched in Apo B-48, consistent with their intestinal origin. Lastly, since each β-VLDL particle contains one copy of Apo B, one can obtain an estimate of the relative Apo E content per β-VLDL particle by calculating for each fraction the densitometric ratio of the Apo E band to the Apo B bands (correcting for the smaller size of Apo B-48 vs. Apo B-100). The results of this analysis are shown in Table I; note that the analysis estimates the relative Apo E/Apo B ratios among the fractions, not the absolute molar ratio of each fraction. The data corroborate previous data (9) and show that the fractions of large β-VLDL (A–C) have a ~4–9-fold higher Apo E/Apo B ratio (i.e., Apo E/particle ratio) than the fractions of smaller β-VLDL (D–F).

The endocytic patterns of the six canine DiI–β-VLDL fractions in mouse peritoneal macrophages are shown in Fig. 3. In this experiment, each of the fractions was incubated with the macrophages for 5 min and then chased in the absence of lipoproteins for 5 min. The cells were then fixed and viewed by fluorescence microscopy (Fig. 3, *A–F*) and phase-contrast microscopy (Fig. 3, *A′–F′*). The micrographs show a marked difference in pattern between the biggest fractions (A and B) and the smallest fractions (E and F): fractions A and B gave a preponderance of widely distributed vesicles (reminiscent of the rabbit β-VLDL patterns shown in reference 37) whereas fractions E and F were mostly central, like the patterns for LDL or α_2M (refer to Fig. 1). Fractions C and D appeared to give patterns that were "mixed" or intermediate between those of the largest and smallest fractions. Thus, the endocytic patterns of large and small canine β-VLDL subfractions differed, and this heterogeneity was most likely the basis for the "mixed" pattern of endocytosis seen with canine holo–β-VLDL.

To quantify these fluorescence microscopy data using a larger number of cells, a double-label study was conducted in which the endocytic patterns of each of the different β-VLDL subfractions were directly compared (that is, in the same cell) to the endocytic pattern of fluorescein-α_2M,

Table I. Percent Composition by Weight and Apo E/Apo B Ratios of Canine Holo–β-VLDL and β-VLDL Subfractions

β-VLDL fraction	% Composition				Densitometric Apo E/Apo B ratio
	Prot	Chol	TG	PL	
Holo	13.2	45.6	21.1	20.1	0.6
Fx A	2.5	38.7	43.2	15.6	3.0
Fx B	5.4	51.2	27.7	15.7	7.1
Fx C	6.8	42.9	30.9	19.4	4.2
Rx D	8.8	42.9	28.0	20.3	0.7*
Fx E	9.4	49.6	14.4	26.6	
Fx F	13.8	50.2	12.4	23.6	

Holo–β-VLDL from cholesterol-fed dogs was isolated, fractionated on BioGel A-150m (see Fig. 2), and analyzed for protein and lipid composition (by weight) as described in Materials and Methods. *Fx*, fraction; *Prot*, protein; *Chol*, cholesterol; *TG*, triglyceride; *PL*, phospholipid.

For the densitometric Apo E/Apo B ratios, canine holo–β-VLDL and fractions A–C, and pooled fractions D–F were subjected to 5–20% SDS-PAGE under reducing conditions and then stained with Coomassie blue and analyzed by densitometry as decribed in detail in Materials and Methods. The densitometric Apo E/Apo B ratio for each of the fractions (as an estimate of the relative Apo E/β-VLDL particle ratios) was calculated as follows: densitometry value of Apo E ÷ (densitometry value of Apo B-100 + 2 × densitometry value of Apo B-48). (The densitometry value of Apo B-48, which is approximately one-half the size of Apo B-100, was multiplied by two to correct for the likelihood that, per molecule, its staining intensity would be about half that of Apo B-100.) The actual densitometry values ($\times 10^{-4}$) of holo–β-VLDL and fractions A–C, and D–F, respectively, were as follows: Apo E = 21.5, 40.0, 44.4, 35.3, 19.7; Apo B-100 = 21.7, 3.1, 1.5, 2.1, 25.4; and Apo B-48 (before multiplying by two) = 8.4, 5.2, 2.4, 3.2, 0.

* Data from pooled fractions D, E, and F.

which, as shown above (see Fig. 1), gives a central pattern of fluorescence like LDL. Macrophages were incubated (5-min pulse/5-min chase) with each of the DiI-labeled canine β-VLDL subfractions plus fluorescein-α_2M and then viewed by fluorescence microscopy. The images (each containing several cells) were then analyzed by digital image processing to determine the percentage of DiI (i.e., β-VLDL) fluorescence intensity or vesicle number that was nonoverlapping in each cell. Thus, a greater degree of nonoverlap with fluorescein-α_2M would be a quantitative measure of the more widely distributed pattern of fluorescence. The data, displayed in Fig. 4, show that fractions A and B had a greater degree of nonoverlap with fluorescein-α_2M than fractions D and F or LDL, whether based upon fluorescence vesicle number (*hatched bars*) or fluorescent intensity (*open bars*). When this analysis was applied to another experiment using a different preparation of DiI-labeled canine β-VLDL subfractions, similar results were obtained. Thus, the quantitative analysis of fluorescent patterns in multiple images corroborated the impressions gained from viewing the fluorescence micrographs in Fig. 3 and demonstrated that canine β-VLDL large subfractions gave a more widely distributed pattern of endocytosis in macrophages than β-VLDL small subfractions.

ACAT-stimulatory Potential of Canine β-VLDL Subfractions

Based upon our previous study comparing the endocytic patterns and ACAT-stimulatory potentials of rabbit β-VLDL and human LDL, a causal relationship between the widely distributed endocytic pattern of rabbit β-VLDL and its high ACAT-stimulatory potential was hypothesized (37). Given

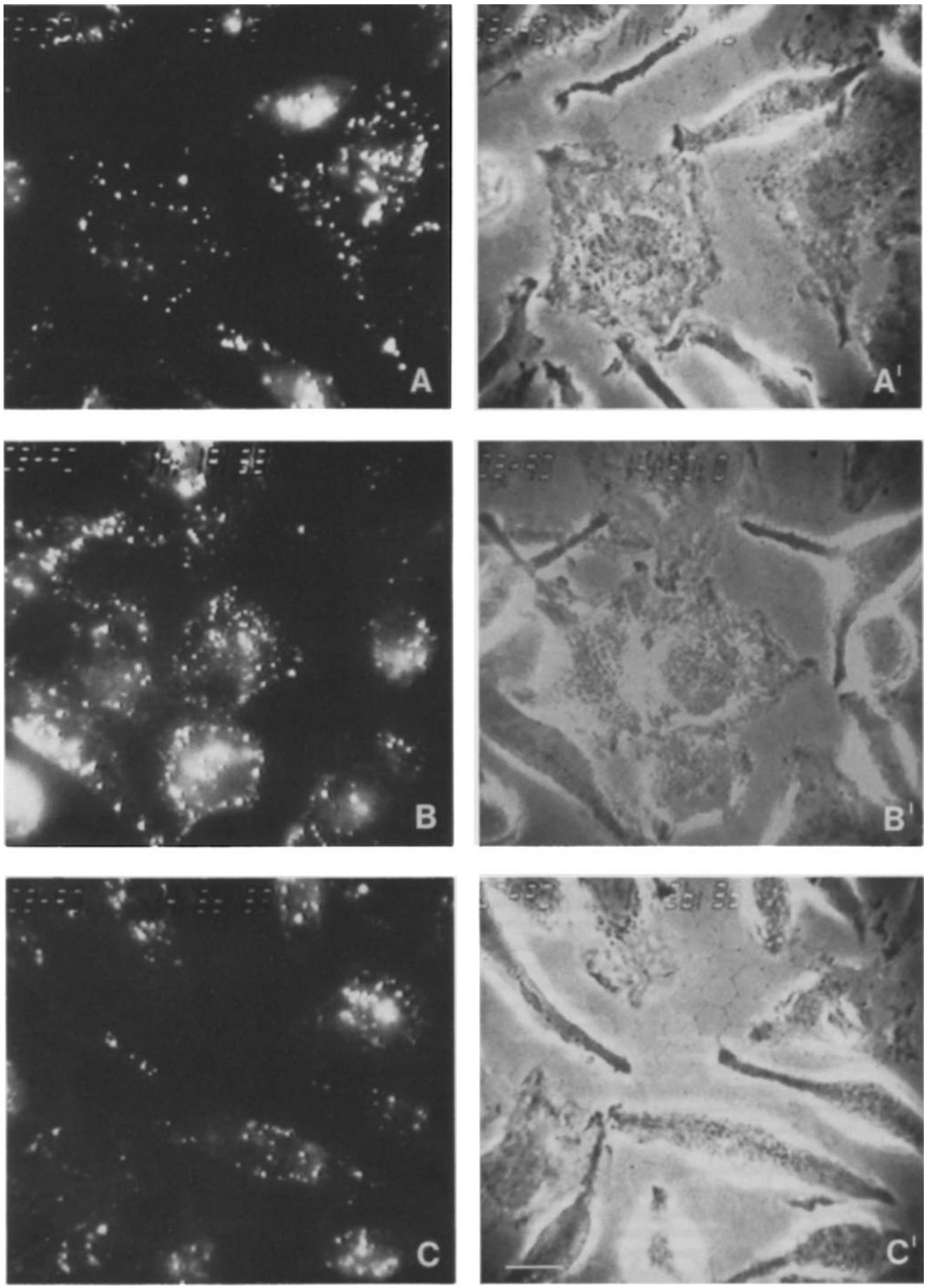

Figure 3. Fluorescence and phase microscopy of macrophages incubated with DiI-labeled canine β-VLDL size subfractions. DiI-labeled β-VLDL subfractions (fraction A [10 μg/ml], fraction B [15 μg/ml], and fractions C–F [25 μg/ml]) from the gel filtration chromatography shown in Fig. 2 were incubated with macrophages for 5 min and then chased in the absence of lipoproteins for 5 min. The cells were fixed and viewed by fluorescence and phase microscopy. *A* refers to macrophages incubated with DiI-labeled fraction A, *B* to fraction B, etc; *A'*, *B'*, etc. refer to the respective phase images of the macrophages incubated with each of the β-VLDL subfractions. Bars, 10 μm.

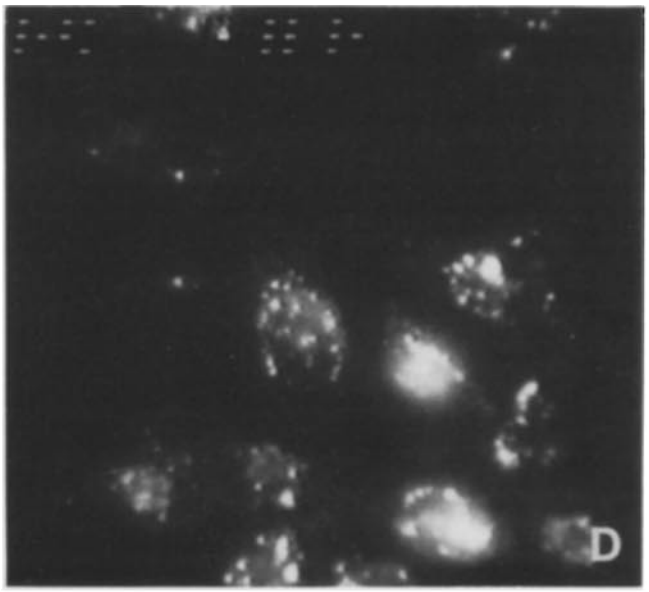
D

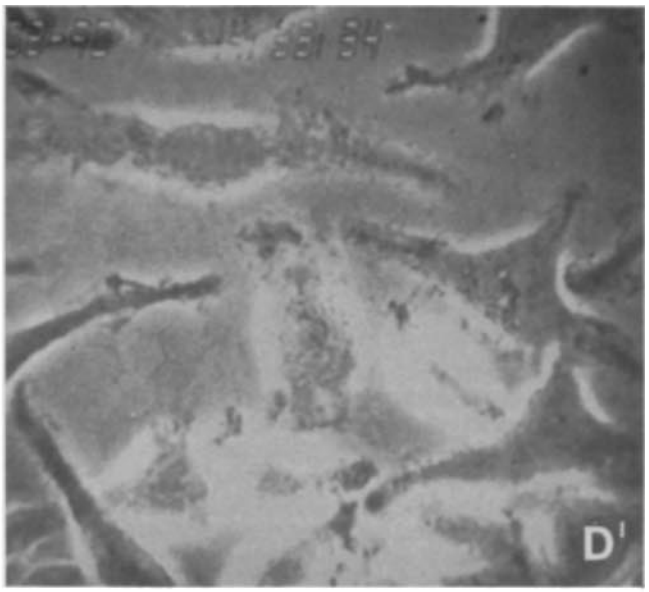
D'

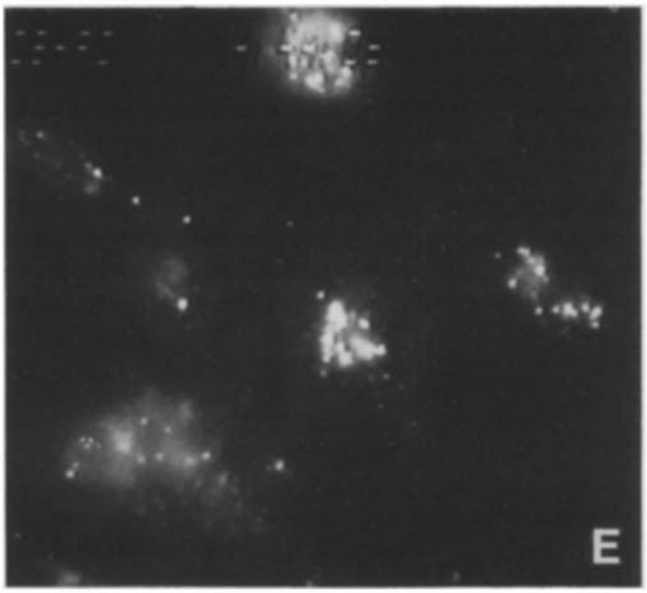
E

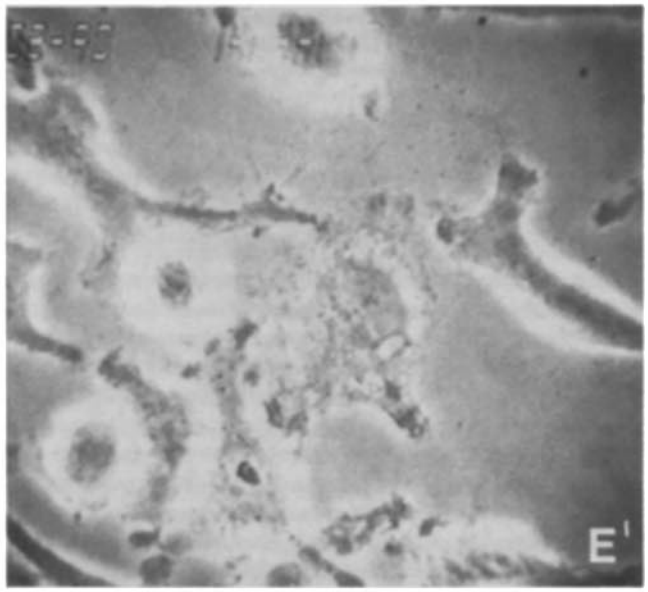
E'

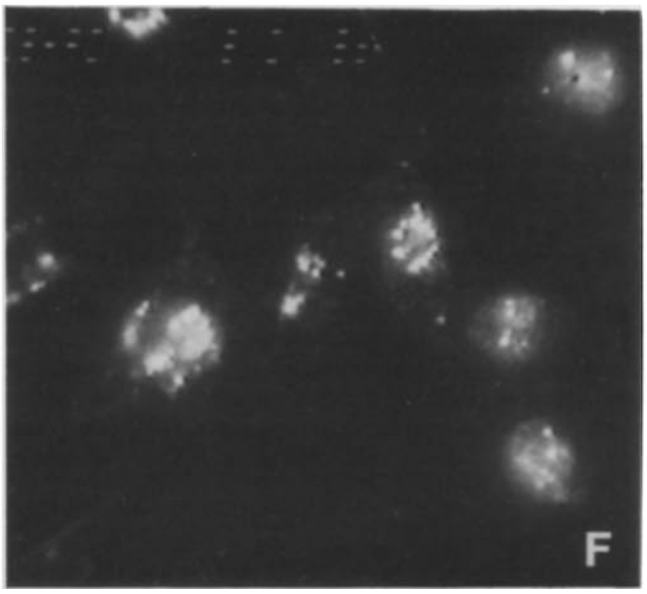
F

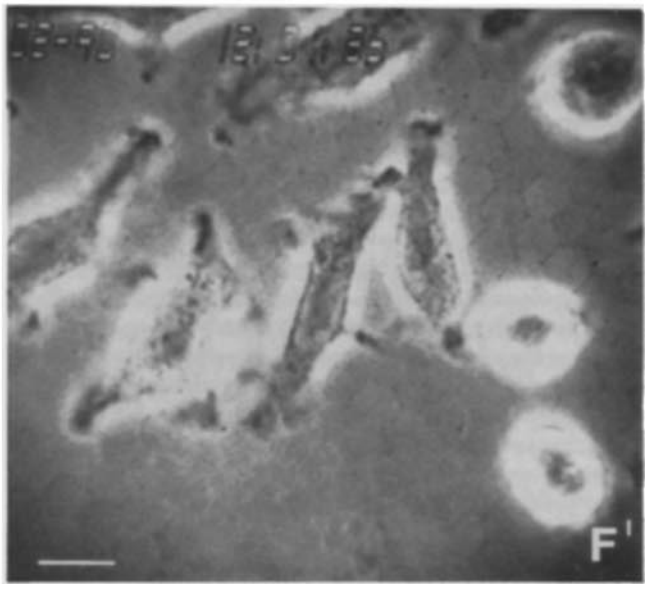
F'

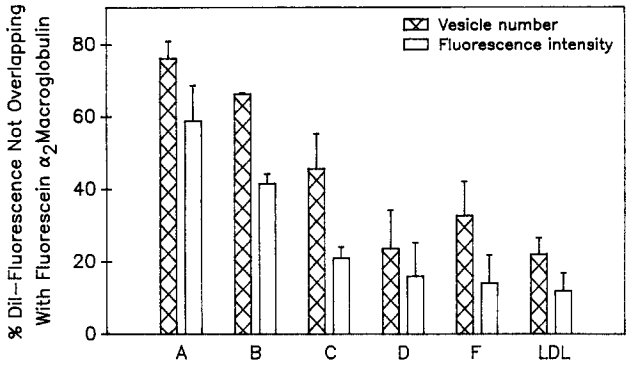

Figure 4. Quantitative analysis of double-label fluorescent images of macrophages incubated with DiI-labeled β-VLDL subfractions (or DiI-LDL) plus fluorescein-α_2M. Macrophages were incubated with DiI-labeled β-VLDL subfractions as described in Fig. 5 (or DiI-LDL [20 μg/ml]) plus fluorescein-α_2M (100 μg/ml) for 5 min and then chased in the absence of lipoproteins for 5 min. The cells were fixed and viewed by video intensification fluorescence microscopy. Two to four image sets (3–5 cells/image) were recorded on videotape, digitized, and analyzed as described. The values shown represent the percentage of nonoverlapping vesicle number and intensity averaged over three or four images, ±SD among the images. *A* refers to data obtained from macrophages incubated with DiI-labeled fraction A, *B* to fraction B, etc; *LDL* refers to data obtained from cells incubated with DiI-LDL. Four fields were analyzed for fraction A, two fields for fractions B and C, three fields for fraction D, and four fields for fraction F and LDL. The total number of endosomes ranged from 279 for fraction C to 1,089 for fraction A.

the different endocytic patterns of canine β-VLDL subfractions (see above), experiments were conducted to determine if there was a correlation between the endocytic targeting and ACAT-stimulatory potential of these subfractions. Therefore, ^{125}I-labeled canine β-VLDL subfractions and canine holo–β-VLDL were incubated with macrophages for 6 h, the last 2 h of which included ^{14}C-oleate, and cellular cholesteryl ^{14}C-oleate was measured to determine ACAT activity (Fig. 5 *A*). The data show that the large subfractions of β-VLDL (i.e., fractions A and B) stimulated ACAT much greater than the smaller subfractions and holo–β-VLDL. However, it was necessary to determine how much of this difference could be explained simply by increased cellular cholesterol delivery by the large β-VLDLs. Therefore, cellular ^{125}I–β-VLDL degradation was assayed (Fig. 5 *B, diagonal hatched bars*), and these protein degradation values were converted into cholesterol delivery values (Fig. 5 *B, open bars*) based upon the cholesterol/protein ratios of each of the subfractions. (This method of estimating β-VLDL–cholesterol delivery to cells has been validated in separate experiments by direct measurements of cholesterol delivery using ^{3}H-CE–labeled β-VLDL [Xu, X., and I. Tabas, unpublished data]). The data show that although the larger subfractions did, in fact, deliver more cholesterol to the cells, this increased delivery could not fully account for the increased ACAT differences. This point is directly illustrated in Fig. 5 *C*, where the values are expressed as an "ACAT activity/cholesterol delivery ratio" to correct ACAT activity differences for differences in cellular cholesterol delivery. The data clearly show that the larger β-VLDL subfractions have a significantly greater ACAT-stimulatory potential than the smaller subfractions. This profile is very similar in appearance to the profile of the quantitative endocytic data for the subfractions shown in Fig.

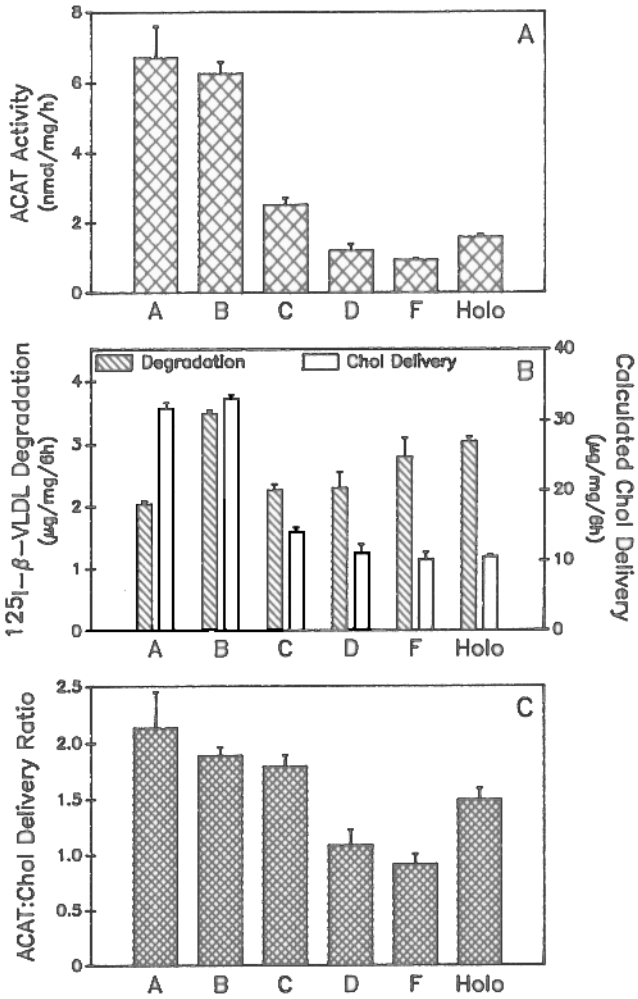

Figure 5. Degradation, estimated cholesterol delivery, and whole cell ACAT activity in macrophages incubated with ^{125}I-labeled β-VLDL subfractions and holo–β-VLDL. DiI-labeled β-VLDL subfractions and holo–β-VLDL (10 μg/ml) were labeled with ^{125}I and incubated with macrophages for 6 h. During the last 2 h of the incubation, ^{14}C-oleate was added to the media (final concentration = 10 mM). The cells were then assayed for ^{14}C-cholesteryl ester content (ACAT activity) (*A*) and the medium was assayed for TCA-soluble ^{125}I-cpm (lipoprotein degradation) (*B, diagonal-hatched bars*). From the protein degradation data and the cholesterol/protein ratio of each fraction, lipoprotein–cholesterol delivery to the cell was calculated (*B, open bars*). The data shown in *C*, which were calculated from the data shown in *A* and *B*, are expressed as the ratio (×10) of ACAT activity (nmol/mg cell protein per h) to lipoprotein–cholesterol delivery (μg/mg per 6 h). Values are means ± SEM (n = 3).

4. Thus, with canine β-VLDL subfractions, as with rabbit β-VLDL vs. LDL, there was a correlation between a widely distributed endocytic pattern and a relatively high ACAT-stimulatory potential.

Mechanisms of Internalization of Canine β-VLDL Subfractions by Mouse Peritoneal Macrophages

Given the distinct endocytic pathway and the large size of fraction A canine β-VLDL and the fact that fraction A β-VLDL constitutes only a small portion of holo-canine β-VLDL (see Fig. 2), it was important to determine whether

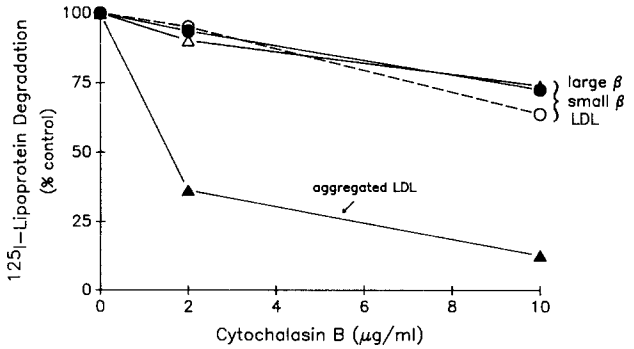

Figure 6. Effect of cytochalasin B on the degradation of ^{125}I-labeled β-VLDL subfractions, LDL, and aggregated LDL. ^{125}I-labeled large canine β-VLDL (fraction A), small canine β-VLDL (fraction F), LDL, and aggregated LDL (10 μg/ml) were incubated with macrophages for 8 h in the absence or presence of the indicated concentrations of cytochalasin B, and ^{125}I-lipoprotein degradation was assayed. The data are expressed as percent degradation by cells in the absence of cytochalasin B (3.2 μg/mg cell protein for fraction A β-VLDL, 2.4 for fraction F β-VLDL, 1.5 for LDL, and 8.9 for aggregated LDL).

the mechanism of uptake by macrophages of Fx *A* (large) β-VLDL was similar to that reported for canine holo-β-VLDL, i.e., receptor-mediated endocytosis via interaction of β-VLDL Apo E molecules with the macrophage's LDL receptor (2, 7, 15, 22). Fluorescence microscopy experiments revealed that both a monoclonal antibody against the receptor-binding region of Apo E and a polyclonal antibody against the ligand-binding region of the LDL receptor each blocked macrophage uptake of the large, as well as small, β-VLDL particles (data not shown). In contrast, a monoclonal antibody against the receptor-binding region of Apo B100 did not block uptake of the large, or small, β-VLDL (data not shown). These data indicated that large β-VLDL, like small β-VLDL and holo-β-VLDL (2, 7, 15, 22), are internalized by macrophages via interaction of the Apo E molecules of the β-VLDL with the macrophage LDL receptor.

The next goal was to determine if the large fraction A particles were internalized by a phagocytic mechanism. In macrophages, phagocytosis is much more susceptible than endocytosis to inhibition by the cytoskeletal inhibitor, cytochalasin B (18, 20). Therefore, the uptake and degradation of ^{125}I-labeled large β-VLDL, small β-VLDL, LDL, and aggregated LDL in mouse peritoneal macrophages, in the absence or presence of cytochalasin B, was measured (Fig. 6). The degradation of ^{125}I-aggregated LDL, which consists of complexes much larger in size than large β-VLDL and which is known to be internalized by macrophages via a phagocytic mechanism (18), was, as expected, inhibited by cytochalasin B (Fig. 6, ▲). In contrast, large β-VLDL (Fig. 6, △), as well as small β-VLDL (●) and LDL (○), demonstrated relative resistance to the inhibitory effects of cytochalasin B. Thus, by this functional definition of phagocytosis, large β-VLDL particles are not internalized by macrophages via a phagocytic mechanism.

The Effect of Partial Antibody-mediated Neutralization of Apo E on the Endocytic Targeting and ACAT-stimulatory Potential of Large β-VLDL

A prominent, distinguishing characteristic of large β-VLDL molecules is that they contain more copies of Apo E per particle than small β-VLDL (see above, Table I, and reference 9). Thus, the possible role of multivalent Apo E in the endocytic targeting and ACAT-stimulatory potential of large β-VLDL was explored. For this purpose, DiI-labeled large β-VLDL was titrated with an amount of anti-Apo E antibody that partially blocked cellular uptake, thereby decreasing the valency of functional Apo E molecules on the particle. This antibody-treated β-VLDL was then compared with control β-VLDL (treated with irrelevant antibody) for endocytic targeting and ACAT-stimulatory potential. For these experiments, a preparation of DiI-labeled rabbit β-VLDL was used which was similar in size, endocytic targeting, ACAT-stimulatory potential, and Apo E content to canine fraction A β-VLDL. (DiI-labeled rabbit β-VLDL was used because it could be more intensely labeled with DiI than fraction A canine β-VLDL, and thus the endocytic pattern of this lipoprotein in the presence of partially blocking amounts of anti-Apo E antibody could be better viewed.)

The endocytic targeting data is shown in Fig. 7. *A* and *B* show a double-label study comparing the endocytic patterns of fluorescein-α_2M and DiI-labeled β-VLDL, respectively, in the same field of cells. As expected, the β-VLDL pattern included numerous widely distributed vesicles that were absent in the central fluorescein-α_2M pattern. Fig. 7, *C* and *D*, shows a similar double-label study comparing the patterns of fluorescein-α_2M and partial anti-Apo E-treated DiI-labeled β-VLDL, respectively. In contrast to the control β-VLDL pattern (above), the antibody-treated β-VLDL pattern was noticeably more central (Fig. 7 *B*), and there was much more overlap with the fluorescein-α_2M pattern (Fig. 7 *C*). (The patterns of the control and anti-Apo E-treated β-VLDLs are of similar brightness since high concentrations of β-VLDL were used [50 μg/ml], thus assuring receptor saturation even with the anti-Apo E-treated β-VLDL.) To prove that the antibody-treated β-VLDL was internalized by the LDL receptor, we showed that the uptake could be blocked by preincubating cholesterol-loaded cells with anti-LDL receptor antibody. The Fc receptor was not involved in the uptake of anti-Apo E-treated β-VLDL since identical results were obtained using Fab fragments generated from the 1D7 antibody (using the quantitative methodology described for Fig. 4, 55 ± 4% of the vesicles from control DiI-labeled β-VLDL images did not overlap with fluorescein-α_2M vesicles, whereas only 28 ± 6% of the vesicles from anti-Apo E Fab-treated DiI-labeled β-VLDL images were nonoverlapping [means ± SD, n = 7 images]). Thus, treatment of large β-VLDL with an amount of anti-Apo E antibody that probably resulted in a decrease in the valency of functional Apo E molecules of the particles led to more central targeting of the β-VLDL.

Based upon the ACAT hypothesis described above, the possibility that this change to a more central pattern was associated with a decrease in the ACAT-stimulatory potential of the antibody-treated β-VLDL was investigated (Fig. 8). Thus, macrophages were incubated with 5 μg/ml control or 10 μg/ml partial anti-Apo E-treated ^{3}H-CE-labeled large β-VLDL for 5 h in the presence of ^{14}C-oleate. Lipid extracts of the cells were assayed for both unesterified and esterified [^{3}H]cholesterol (β-VLDL-cholesterol in cells; *open bars*) and for cholesteryl ^{14}C-oleate (ACAT-derived CE; cross-hatched bars). (Under the conditions of this experiment, <10% of the β-VLDL-cholesterol delivered to the cells is excreted to the medium [our unpublished data]). The

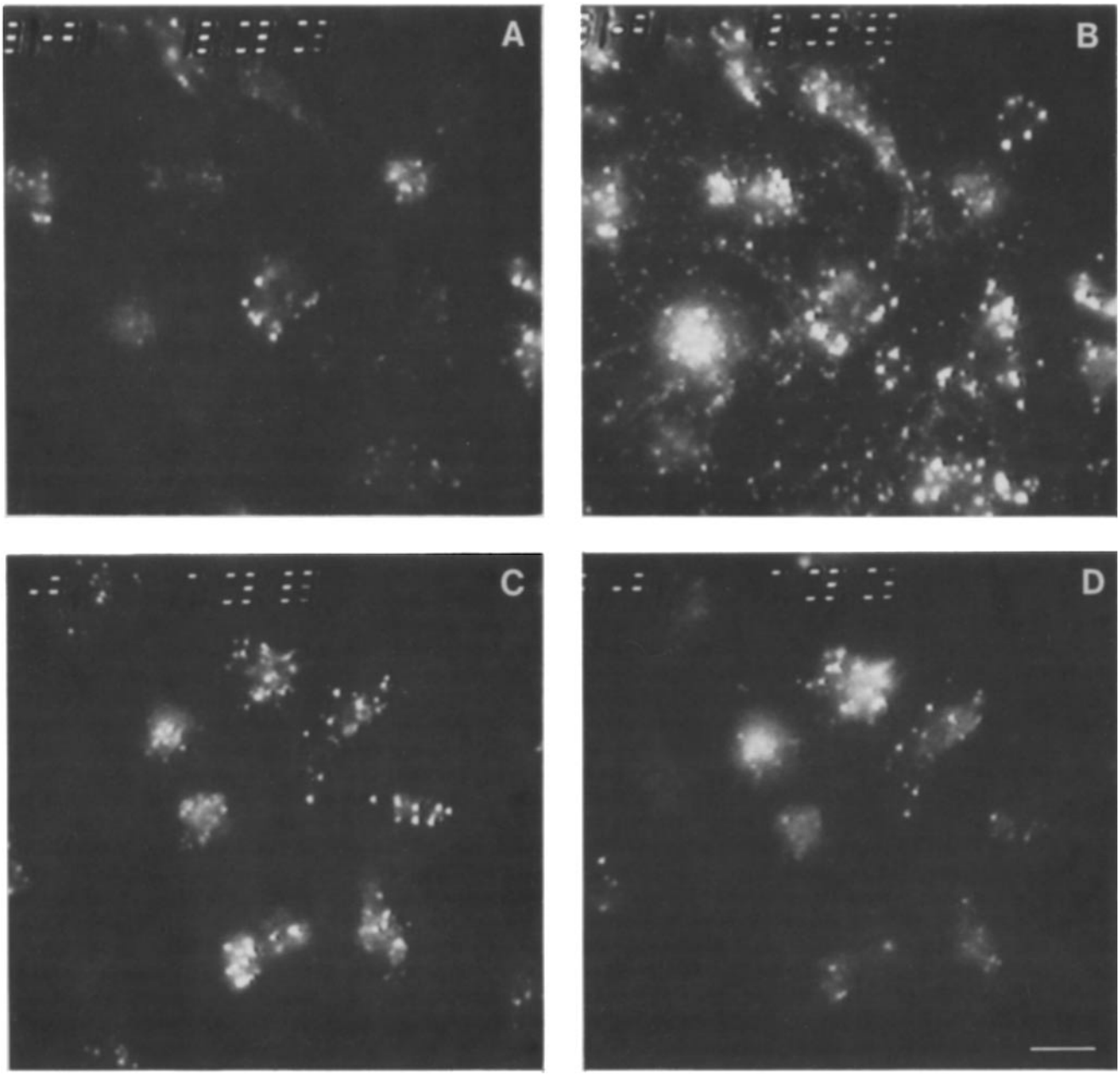

Figure 7. Effect of partial anti-Apo E treatment of large β-VLDL on its endocytic targeting in macrophages. In the double-label experiment shown in *A* and *B*, macrophages were incubated (6-min pulse/4-min chase) with 50 μg/ml DiI-labeled large rabbit β-VLDL (preincubated with 50 μg/ml of an control antibody) plus 100 μg/ml fluorescein-α_2M. The cells were then fixed and viewed for fluorescein (*A*) and DiI (*B*). In the experiment shown in *C* and *D*, a similar protocol was used except 50 μg/ml DiI-labeled β-VLDL was preincubated with 50 μg/ml anti-Apo E antibody before incubation (plus fluorescein-α_2M) with macrophages. The fluorescein (α_2M) pattern is shown in *C* and the DiI (β-VLDL) pattern is shown in *D*. Bar, 10 μm.

data show that partial anti-Apo E treatment of β-VLDL led to a twofold decrease in ACAT-derived CE under conditions in which the lipoprotein-cholesterol delivered to the cells was similar. Thus, anti-Apo E treatment of large β-VLDL changed both the endocytic pattern and the ACAT-stimulatory potential of the lipoprotein, furthering the correlation between a widely distributed endocytic pattern and a high ACAT-stimulatory potential.

The pH-dependent Release of Large and Small Canine β-VLDL from Macrophage Surface LDL Receptors

The endocytic pathway for LDL, like that for many other endocytosed ligands, involves an acid-dependent dissociation of ligand from receptor in the sorting endosome; the ligand is then targeted to lysosomes, and the receptor is targeted to the plasma membrane via a recycling pathway (13). Thus, part of the basis for the different endocytic targeting of small β-VLDL (to perinuclear lysosomes) and large β-VLDL (to more widely distributed vesicles) might be a difference in acid-mediated ligand-receptor dissociation for the two β-VLDLs in the sorting endosome. For instance, if the large β-VLDL were more resistant to acid-mediated ligand-receptor dissociation, less of the β-VLDL would be released from its receptor and delivered to perinuclear lysosomes. As an

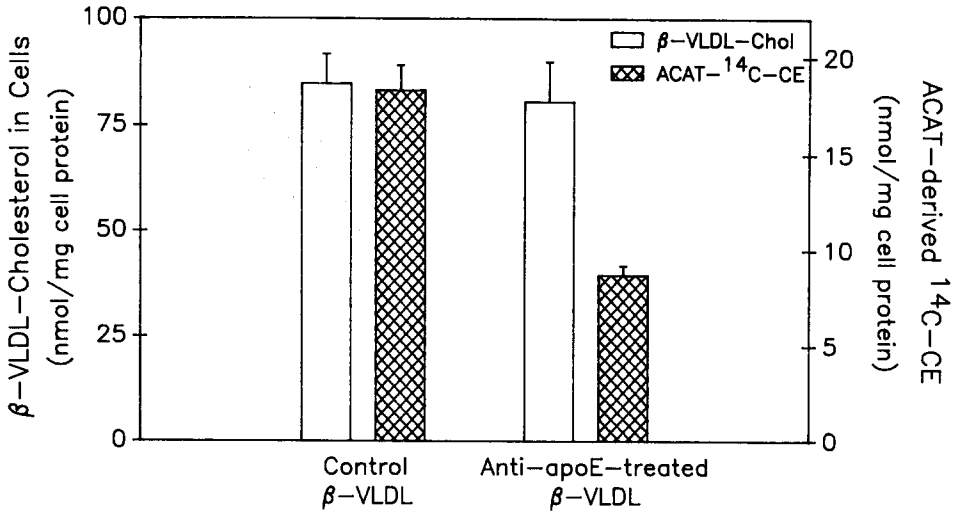

Figure 8. Effect of partial anti-Apo E treatment of large β-VLDL on its ACAT-stimulatory potential in macrophages. ^{3}H-CE-labeled large rabbit β-VLDL (10 μg/ml; 725 cpm/nmol) was preincubated with 5 μg/ ml control antibody (*Control* β-VLDL) or with 5 μg/ml anti-Apo E antibody (Anti-Apo E-treated β-VLDL). The control β-VLDL, diluted twofold with culture medium (final concentration = 5 μg/ml), and the undiluted anti-Apo E-treated β-VLDL (10 μg/ml) were incubated with cells for 5 h in the presence of 10 mM ^{14}C-oleate. The culture medium was then removed, and the cells were washed and incubated with DME/0.2% BSA in the absence of lipoproteins for 30 min so that any surface bound ^{3}H-CE-β-VLDL would be internalized by the cells (37). Lipid extracts of the cells were then analyzed by TLC for unesterified and esterified [^{3}H]cholesterol and for cholesteryl ^{14}C-oleate. Values are means ± SEM (n = 3).

initial test of this idea, ^{125}I-labeled fraction F (*small*) or A (*large*) canine β-VLDL was incubated with macrophages at 4°C for 3 h at pH 7.4. The cells were then washed, and individual monolayers were incubated at 4°C for 20 min in buffered solutions ranging in pH from 7.0 to 5.0. Cell-associated and media ^{125}I were measured to determine the percent release of ligand from the cell surface receptors (Fig. 9 *A*). The data clearly show a difference in the release of large and small β-VLDL's: small β-VLDL (*Fx F*; ○) was progressively released from cell surface receptors as the pH was lowered from 7.0 to 5.0. Similar results were found with LDL (data not shown). In contrast, large β-VLDL (*Fx A*; ●) showed a marked resistance to acid-mediated release from the receptors.

To further explore this idea, an experiment was designed to determine whether partial anti-Apo E treatment of β-VLDL, which changes its endocytic targeting to a more central pattern (see above and Fig. 7), resulted in an increase in the acid-dependent release of the β-VLDL from its receptor. As shown in Fig. 9 *B*, ^{125}I-labeled large rabbit β-VLDL was treated in the absence or presence of two concentrations of anti-Apo E Fab (weight ratios of Fab to ^{125}I-β-VLDL protein = 5:1 and 12.5:1, respectively). Macrophages were then incubated at 4°C with the untreated and Fab-treated ^{125}I-β-VLDLs, and then the cells were postincubated (at 4°C) in pH 5.5 buffer; the relative amounts of cell-associated and released ^{125}I-β-VLDL were determined. The data show that anti-Apo E Fab treatment of β-VLDL resulted, in a dose-dependent manner, in a greater release of ^{125}I-β-VLDL from cell surface receptors at pH 5.5. Thus, a functional decrease in β-VLDL-Apo E valency by partial anti-Apo E treatment resulted in both a more central endocytic pattern (see Fig. 7) and an increase in acid-mediated release from cell surface receptors (see Fig. 9 *B*). These findings support the hypothesis that multivalent Apo E on large β-VLDL particles, perhaps through receptor cross-linking, results in decreased dissociation of the particles from their receptors in acidic sorting endosomes, which, in turn, may contribute to their targeting to widely distributed vesicles in mouse peritoneal macrophages.

Discussion

In our previous study, rabbit β-VLDL and human LDL, despite being internalized by the same receptor, were shown to have divergent endocytic pathways in mouse peritoneal macrophages (37). A major goal resulting from that study was to determine the properties of β-VLDL important in its divergent pattern of endocytosis. The current study has approached this issue by first showing that the widely distributed pattern of endocytosis characteristic of rabbit β-VLDL was seen only with the large, intestinally derived subfraction of canine β-VLDL. (Subsequently, most of our rabbit β-VLDL preparations were shown to be heavily enriched in Apo E-rich, large β-VLDL [our unpublished data], thus explaining why these preparations of holo-β-VLDL from rabbit gave a mostly widely distributed pattern.) With this finding, the specific properties of large β-VLDL, distinct from those of small β-VLDL, that might be responsible for the widely distributed pattern of endocytosis could be investigated.

Since most of canine holo-β-VLDL is made up of small β-VLDL (Fig. 2), one possibility not ruled out by previous studies with holo-β-VLDL from dogs was that large β-VLDL particles were internalized by a different receptor or different mechanism from small β-VLDL. In particular, given the very large size of the large β-VLDL particles, there was a possibility that these particles were phagocytosed by the macrophages. However, the cytochalasin B experiment (Fig. 6) showed that the uptake was relatively resistant to disruption of the actin cytoskeleton, thus indicating that uptake by a classical phagocytosis mechanism was unlikely (18, 20). Furthermore, the uptake of the large particles, like that of canine holo-β-VLDL (2, 7, 15, 22), was dependent upon Apo E of the β-VLDL interacting with the macrophage's LDL receptor (see text). In particular, the fact that an LDL receptor antibody blocked particle uptake and thiol ester-cleaved α_2-macroglobulin did not block uptake (data not shown; see reference 16) indicated that the LDL receptor-related protein/α_2-macroglobulin receptor (23) was not involved in the uptake of large β-VLDL. From these combined data, we concluded that the divergence in endocytosis be-

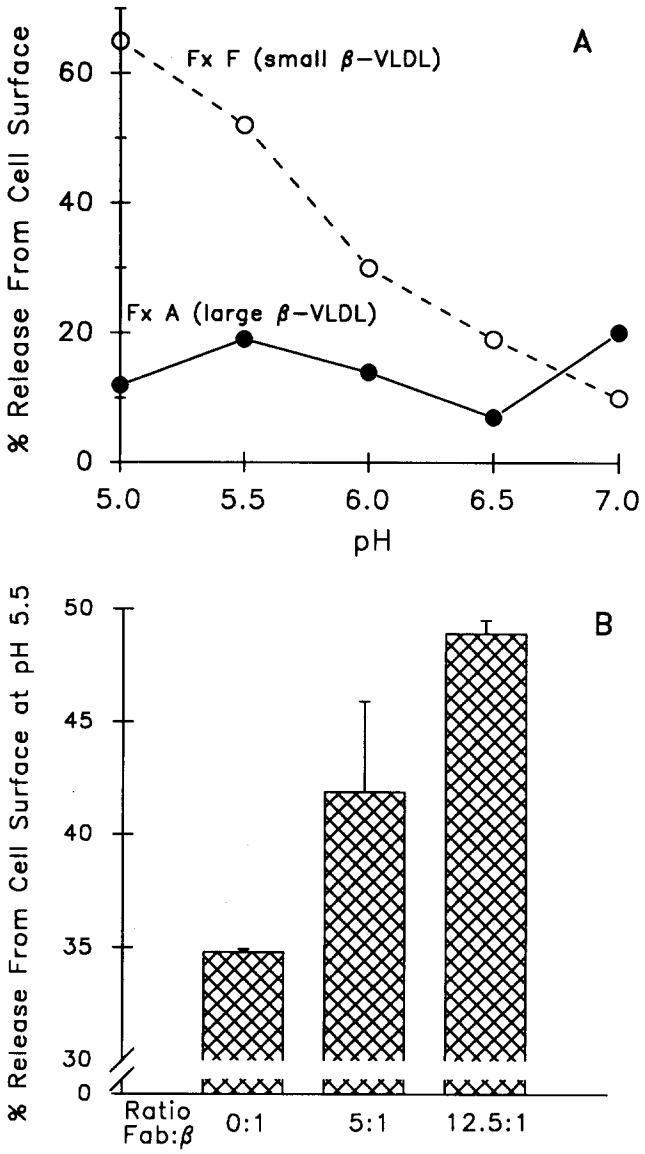

Figure 9. The effect of β-VLDL particle size and anti–Apo E Fab treatment on the pH-dependent release of β-VLDL from macrophage cell surface receptors. In *A*, ^{125}I-labeled fraction A (●) or fraction F canine β-VLDL (○) (4 μg/ml) was incubated with macrophages at 4°C for 3 h in DME/25 mM Hepes (pH 7.4)/10% lipoprotein-deficient serum. The cells were then washed with PBS/0.2% BSA and incubated with 50 mM NaCl/5% lipoprotein-deficient serum containing 50 mM Tris-succinate (pH 5.0 or 5.5) or 50 mM Tris-maleate (pH 6.0, 6.5, or 7.0) for 20 min at 4°C. Cell-associated and media ^{125}I-cpm were measured, and the data are expressed as ^{125}I-cpm in the medium as a percent of total (i.e., medium + cell-associated) ^{125}I-cpm. In *B*, 10 μg/ml ^{125}I-labeled large rabbit β-VLDL was incubated for 1 h at 37°C in the absence or presence of 50 or 125 μg/ml anti-Apo-E Fab (indicated, respectively, as Ratio Fab:β = 0:1, 5:1, or 12.5:1). The labeled β-VLDLs were subject to the same acid-release experiment described for *A* except that only pH 7.0 and 5.5 buffers were used. The pH 5.5 percent release data is shown. The total ^{125}I-β-VLDL originally bound to the cells before addition of buffer (i.e., buffer-released plus cell-associated) was 115.8 ± 5.4, 111.1 ± 7.3, and 114.6 ± 3.2 ng/mg cell protein for the three Fab:β ratios, respectively. The percent releases at pH 7.0 for Fab:β ratios of 0:1 and 12.5:1 were, respectively, 33.2 ± 0.1% and 31.6 ± 0.1%. When a nonimmune Fab was used at a ratio of 12.5:1, the values were the same as those obtained in the absence of Fab (i.e., ratio 0:1). Values are means ± SEM (n = 3).

tween large vs. small β-VLDL was not due to phagocytosis of the large particles or binding to different receptors.

Another possibility to explain the endocytic divergence was particle size itself. The diameter of large β-VLDL particles (see Fig. 2, *inset*) is similar to or larger than the diameters of coated pits and endocytic vesicles, and it is conceivable that a vesicle loaded to capacity with one large particle may undergo alternative routing due to changes in the interaction or fusion of the vesicle with other cellular organelles. However, the finding that partial anti–Apo E treatment of large β-VLDL resulted in the particles' being targeted more centrally (see Fig. 7) demonstrates that large particle size alone is not sufficient for targeting to widely distributed vesicles.

A third possibility for the endocytic divergence is related to the greater number of Apo E molecules per large β-VLDL (vs. small β-VLDL) that might result in differences in β-VLDL–receptor interactions. An important role for multiple Apo E's is suggested by the data in Fig. 7, which shows that functional depletion of Apo E molecules on large β-VLDL by titration with anti–Apo E antibody leads to an almost total elimination of targeting to widely distributed vesicles. An attractive hypothesis relating Apo E and endocytic targeting is that the multivalent Apo E on large β-VLDL might lead to a greater degree of receptor cross-linking than those on small β-VLDL, which, in turn, may be responsible for the greater resistance of the large β-VLDL to acid-mediated release from receptors (see Fig. 9). If there is diminished acid-induced ligand–receptor dissociation in the acidic sorting endosome, the normal rapid delivery of dissociated ligand to perinuclear lysosomes would not occur as completely as it does with small β-VLDL, LDL, or α_2M. Instead, a substantial portion of the β-VLDL would possibly end up in recycling endosomes (like transferrin [5, 21]) or some other vesicles distal to sorting endosomes. Attempts to colocalize large β-VLDL and transferrin have been unsuccessful because of the low amount of uptake of transferrin in mouse peritoneal macrophages. In addition, we have been unable to detect significant recycling of internalized β-VLDL (our unpublished data). Thus, the actual identity and fate of the β-VLDL–containing vesicles must await further experimentation.

Previous work has indicated that receptor cross-linking can block ligand–receptor recycling. Hopkins and Trowbridge (14) showed that multivalent transferrin on gold particles was targeted first to multivesicular bodies and then to lysosomes in human carcinoma A431 cells instead of being recycled like univalent transferrin. Similarly, Weissman et al. (38) found that exposure of human erythroleukemia K562 cells to a divalent antitransferrin receptor antibody blocked receptor recycling, perhaps through receptor cross-linking. Mellman and Plutner (26) demonstrated that Fc receptors on J774 cells and thioglycollate-elicited mouse peritoneal macrophages were recycled when exposed to monovalent ligands but were delivered to lysosomes when exposed to polyvalent IgG complexes. Other receptors whose recycling was blocked by polyvalent antibodies include the LDL receptor on human fibroblasts (1), the insulin receptor on IM-9 lymphocytes (32), and the cation-independent (215-kD) phosphomannosyl receptor on human fibroblasts (29). In several of the examples above, the multivalent-bound receptors were targeted to lysosomes. Interestingly, however, the intracellular distribution of phosphomannosyl receptors changed from

their normal juxtanuclear site to a more peripheral distribution upon addition of polyvalent antibody (29). The hypothesis put forth here is that LDL receptor cross-linking on mouse peritoneal macrophages (i.e., by "multivalent" large β-VLDL) changes endocytic targeting on the ligand from a lysosomal distribution to, at least initially, a more widely distributed pattern. The explanation of why, in our case, putative receptor cross-linking leads to a more peripheral endocytic, and less lysosomal, pattern awaits further investigation into the nature of the β-VLDL–containing vesicles, the eventual fate of β-VLDL in our cells, and the targeting of lipoproteins such as β-VLDL in different cell types. Nonetheless, the possibility that LDL receptor cross-linking by large β-VLDL results in its endocytic divergence from small β-VLDL and LDL may represent an important physiological example of the effect of receptor cross-linking on endocytic targeting.

The original impetus for our previous study on the divergent endocytic pathways of β-VLDL and LDL in mouse peritoneal macrophages was a hypothesis which attempted to explain the greater ability of β-VLDL to stimulate ACAT in these cells (37). According to this hypothesis, the targeting of β-VLDL to a set of vesicles distinct from those of LDL would lead to a greater stimulation of ACAT by the β-VLDL. The actual mechanism might involve a physical association of the β-VLDL–containing vesicles with ACAT (or proximity to the enzyme). Alternatively, the β-VLDL–containing vesicles may possess some property, such as increased ability to transfer cholesterol, that would lead to increased ACAT stimulation. Although the current study does not directly address these possible mechanisms, the data continue to support the overall hypothesis linking endocytic targeting with ACAT stimulation. For instance, large β-VLDL are targeted in a more widely distributed pattern than small β-VLDL (see Figs. 3 and 4) and also have a higher ACAT stimulatory potential than the smaller particles (see Fig. 5). Similarly, the partial anti-Apo E treatment of β-VLDL changed its targeting to a more central pattern (see Fig. 7) and also decreased its ability to stimulate ACAT (see Fig. 8). Thus, the study strengthens the correlation between the targeting of β-VLDL to widely distributed vesicles and high ACAT stimulation and therefore further supports the causal nature of this relationship.

The widely distributed endocytic pattern and high ACAT-stimulatory potential of large β-VLDL may have particular relevance to our understanding of atherogenesis. Large β-VLDL, which is intestinally derived, has structural and metabolic properties similar to those of postprandial chylomicron remnants (9), which may be a relatively common atherogenic particle in man (39). Thus, by studying in detail the pathways and metabolism of these particles in macrophages, the cell type that leads to atheroma foam cells (8, 10, 34), further insight into their association with atherogenesis may be gained. Although our current hypothesis has focused on the relationship between the endocytic pathway of these particles and ACAT stimulation, it is possible that other or additional consequences of the pathway (e.g., specific proteolytic processing of the proteins or catabolism of the lipids of large β-VLDL) may be revealed and shown to be physiologically important.

We are grateful to Nanda Beatini and Laura Morse for providing technical assistance.

This work was supported by National Institute for Health grants (HL-39703 and HL-21006; Ira Tabas), HL-41633; Thomas L. Innerarity, and DK-27083; Frederick R. Maxfield. Ira Tabas is an Established Investigator of the American Heart Association and Boehringer-Ingelheim, Inc.

Received for publication 26 June 1991 and in revised form 9 August 1991.

References

1. Anderson, R. G. W., M. S. Brown, U. Beisiegel, and J. L. Goldstein. 1982. Surface distribution and recycling of the LDL receptor as visualized by anti-receptor antibodies. *J. Cell Biol.* 93:523–551.
2. Bates, S. R., B. A. Coughlin, T. Mazzone, J. Borensztajn, and G. S. Getz. 1987. Apoprotein E mediates the interaction of β-VLDL with macrophages. *J. Lipid Res.* 28:787–797.
3. Beisiegel, U., T. Kita, R. G. W. Anderson, W. J. Schneider, M. S. Brown, and J. L. Goldstein. 1981. Immunologic cross-reactivity of the low density lipoprotein receptor from bovine adrenal cortex, human fibroblasts, canine liver and adrenal gland, and rat liver. *J. Biol. Chem.* 256:4071–4078.
4. Boyles, J. K., C. D. Zoellner, L. J. Anderson, L. M. Kosik, R. E. Pitas, K. H. Weisgraber, D. Y. Hui, R. W. Mahley, P. J. Gebicke-Haerter, M. J. Ignatius, and E. M. Shooter. 1989. A role for apolipoprotein E, apolipoprotein A-1, and low density lipoprotein receptors in cholesterol transport during regeneration and remyelination of the rat sciatic nerve. *J. Clin. Invest.* 83:1015–1031.
5. Dautry-Varsat, A., A. Ciechanover, and H. F. Lodish. 1983. pH and the recycling of transferrin during receptor-mediated endocytosis. *Proc. Natl. Acad. Sci. USA.* 80:2258–2262.
6. Dunn, K. W., T. E. McGraw, and F. R. Maxfield. 1989. Iterative fractionation of recycling receptors from lysosomally destined ligands in an early sorting endosome. *J. Cell Biol.* 109:3303–3314.
7. Ellsworth, J. L., F. B. Kraemer, and A. D. Cooper. 1987. Transport of β-VLDL and chylomicron remnants by macrophages is mediated by the LDL receptor pathway. *J. Biol. Chem.* 262:2316–2325.
8. Faggioto, A., R. Ross, and L. Harker. 1984. Studies of hypercholesterolemia in the nonhuman primate. I. Changes that lead to fatty streak formation. *Arteriosclerosis.* 4:323–340.
9. Fainaru, M., R. W. Mahley, R. L. Hamilton, and T. L. Innerarity. 1982. Structural and metabolic heterogeneity of β-very low density lipoproteins from cholesterol-fed dogs and from humans with type III hyperlipoproteinemia. *J. Lipid Res.* 23:702–714.
10. Gerrity, R. G. 1991. The role of the monocyte in atherogenesis. I. Transition of blood-borne monocytes into foam cells in fatty lesions. *Am. J. Pathol.* 103:181–190.
11. Goldstein, J. L., Y. K. Ho, S. K. Basu, and M. S. Brown. 1979. Binding site on macrophages that mediates uptake and degradation of acetylated low density lipoprotein producing massive cholesterol deposition. *Proc. Natl. Acad. Sci. USA.* 76:333–337.
12. Goldstein, J. L., S. K. Basu, and M. S. Brown. 1983. Receptor-mediated endocytosis of low density lipoprotein in cultured cells. *Methods Enzymol.* 98:241–260.
13. Goldstein, J. L., M. S. Brown, R. G. W. Anderson, D. W. Russell, and W. J. Schneider. 1985. Receptor-mediated endocytosis: concepts emerging from the LDL receptor system. *Annu. Rev. Cell Biol.* 1:1–39.
14. Hopkins, C. R., and I. S. Trowbridge. 1983. Internalization and processing of transferrin and the transferrin receptor in human carcinoma A431 cells. *J. Cell Biol.* 97:508–521.
15. Hui, D. Y., T. L. Innerarity, and R. W. Mahley. 1984. Defective hepatic lipoprotein receptor binding of β-very low density lipoproteins from type III hyperlipoproteinemic patients. Importance of apolipoprotein E. *J. Biol. Chem.* 259:860–869.
16. Hussain, M. M., F. R. Maxfield, J. Más-Oliva, I. Tabas, Z-S. Ji, T. L. Innerarity, and R. W. Mahley. 1991. Clearance of chylomicron remnants by the low density lipoprotein receptor-related protein/α_2-macroglobulin receptor. *J. Biol. Chem.* 266:13936–13940.
17. Innerarity, T. L., R. E. Pitas, and R. W. Mahley. 1982. Modulating effects of canine high density lipoproteins on cholesteryl ester synthesis induced by β-very low density lipoproteins in macrophages. Possible *in vitro* correlates with atherosclerosis. *Arteriosclerosis.* 2:114–124.
18. Khoo, J. C., E. Miller, P. McLoughlin, and D. Steinberg. 1988. Enhanced macrophage uptake of low density lipoprotein after self-aggregation. *Arteriosclerosis.* 8:348–358.
19. King, J., and U. K. Laemmli. 1971. Polypeptides of the tail fibers of bacteriophage T4. *J. Mol. Biol.* 62:465–477.
20. Klaus, G. G. 1973. Cytochalasin B; dissociation of pinocytosis and phagocytosis by peritoneal macrophages. *Exp. Cell Res.* 79:73–78.
21. Klausner, R. D., G. Ashwell, J. van Renswoude, J. B. Harford, and K. R. Bridges. 1983. Binding of apotransferrin to K562 cells: explanation of the transferrin cycle. *Proc. Natl. Acad. Sci. USA.* 80:2263–2266.
22. Koo, C., M. E. Wernette-Hammond, and T. L. Innerarity. 1986. Uptake of canine β-very low density lipoproteins by mouse peritoneal macrophages is mediated by a low density lipoprotein receptor. *J. Biol. Chem.* 261:11194–11201.
23. Kowal, R. C., J. Herz, J. L. Goldstein, V. Esser, and M. S. Brown. 1989.

Low density receptor-related protein mediates uptake of cholesteryl esters derived from apoprotein E-enriched lipoproteins. *Proc. Natl. Acad. Sci. USA.* 86:5810–5814.
24. Lowry, O. H., N. J. Rosenbrough, A. L. Farr, and R. J. Randall. 1951. Protein measurement with the folin phenol reagent. *J. Biol. Chem.* 193:265–275.
25. Mahley, R. W., T. L. Innerarity, M. S. Brown, Y. K. Ho, and J. L. Goldstein. 1980. Cholesterol ester synthesis in macrophages: stimulation by β-very low density lipoproteins from cholesterol-fed animals of several species. *J. Lipid Res.* 21:970–980.
26. Mellman, I., and H. Plutner. 1984. Internalization and degradation of macrophage Fc receptors bound to polyvalent immune complexes. *J. Cell Biol.* 98:1170–1177.
27. Milne, R. W., P. Douste-Blazy, Y. L. Marcel, and L. Retegui. 1981. Characterization of monoclonal antibodies against human apolipoprotein E. *J. Clin. Invest.* 68:111–117.
28. Milne, R. W., R. Theolis, Jr., R. B. Verdery, and Y. L. Marcel. 1983. Characterization of monoclonal antibodies against human low density lipoprotein. *Arteriosclerosis.* 3:23–30.
29. Nolan, C M., K. E. Creek, J. H. Grubb, and W. S. Sly. 1987. Antibody to the phosphomannosyl receptor inhibits recycling of receptor in fibroblasts. *J. Cell. Biochem.* 35:137–151.
30. Pitas, R. E., T. L. Innerarity, and R. W. Mahley. 1991. Foam cells in explants of atherosclerotic rabbit aortas have receptors for β-very low density lipoproteins and modified low density lipoproteins. *Arteriosclerosis.* 3:2–12.
31. Ross, A. C., K. J. Go, J. G. Heider, and G. H. Rothblatt. 1984. Selective inhibition of acyl coenzyme A:cholesterol acyltransferase by compound 58-035. *J. Biol. Chem.* 259:815–819.
32. Roth, R. A., B. A. Maddux, D. J. Cassell, and I. D. Goldfine. 1983. Regulation of the insulin receptor by a monoclonal anti-receptor antibody: evidence that receptor down regulation can be independent of insulin action. *J. Biol. Chem.* 258:12094–12097.
33. Salzman, N. H., and F. R. Maxfield. 1989. Fusion accessibility of endocytic compartments along the recycling and lysosomal endocytic pathways in intact cells. *J. Cell Biol.* 109:2097–2104.
34. Schaffner, T., K. Taylor, E. Bartucci, K. Fischer-Dzoga, J. Beeson, S. Glagov, and R. Wissler. 1980. Arterial foam cells with distinctive immunomorphologic and histochemical features of macrophages. *Am. J. Pathol.* 100:57–73.
35. Schneider, W. J., S. K. Basu, M. J. McPhaul, J. L. Goldstein, and M. S. Brown. 1979. Solubilization of the low density lipoprotein receptor. *Proc. Natl. Acad. Sci. USA.* 76:5577–5581.
36. Tabas, I., D. A. Weiland, and A. R. Tall. 1985. Unmodified low density lipoprotein causes cholesteryl ester accumulation in J774 macrophages. *Proc. Natl. Acad. Sci. USA.* 82:416–420.
37. Tabas, I., S. Lim, X. Xu, and F. R. Maxfield. 1990. Endocytosed β-VLDL and LDL are delivered to different intracellular vesicles in mouse peritoneal macrophages. *J. Cell Biol.* 111:929–940.
38. Weissman, A. M., R. D. Klausner, K. Rao, and J. B. Harford. 1986. Exposure of K562 cells to anti-receptor monoclonal antibody OKT9 results in rapid redistribution and enhanced degradation of the transferrin receptor. *J. Cell Biol.* 102:951–958.
39. Zilversmit, D. B. 1979. Atherogenesis: a postprandial phenomenon. *Circulation.* 60:473–485.